

Mechanical anisotropy induced by drying shrinkage: modeling and experiment

N.Burlion, F.Bourgeois & J.F.Shao

Laboratory of Mechanics of Lille, USTL-EUDIL, Villeneuve d'Ascq, France

ABSTRACT: This paper is devoted to experimental investigation and numerical modelling of induced anisotropic damage in concrete during drying shrinkage. In the first part, a summary of experimental result is presented. A prismatic bar is subjected to drying process through its four lateral faces during one year. A cubic sample is then cut from the prism and submitted to hydrostatic compression. Strains in three orthogonal orientations are measured by strain gauges glued on six faces of the cube. The results clearly show anisotropic deformations between the orientations which are respectively parallel and perpendicular to principal desiccation direction. In the second part, an elastoplastic damage model is proposed. A second rank tensor is used to describe orientation and density of microcracks. The effective elastic properties of damaged material are derived from a suitable form of free energy function, which is based on micromechanics analysis. A pragmatic damage criterion is proposed so that the damage evolution is related to tensile elastic and plastic strains. Simulation of laboratory tests show that the model is able to describe basic characteristics of induced anisotropic behaviour of concrete. A simple application example is finally provided.

1 INTRODUCTION

Many concrete structures are submitted to coupled actions of mechanical loading, drying and wetting processes and temperature variation. Elaboration of reliable modelling of concrete behaviour under such coupled actions is very complex. The purpose of this work is to study one important feature of these coupled phenomena, effect of desiccation shrinkage on mechanical behaviour of concrete. Indeed, in spite of studies available so far on estimation of shrinkage deformation of concrete, it exists few results concerning effects of drying shrinkage on mechanical behaviour of concrete. In particular, variation of moisture content due to drying or wetting may be responsible of concrete damage by initiation and growth of microcracks (Wittmann 1997). Further, induced material damage is usually anisotropic in nature, due to oriented distribution of microcracks. Therefore, we propose a constitutive modelling of material behaviours in saturated and unsaturated conditions, by coupling elastoplastic deformation and anisotropic damage. During the last thirty years, many advances have been performed for unsaturated soils and clays both in experimental investigation and constitutive modelling, for instance Alonso et al. (1987, 1990). However, significant efforts are still

necessary for modelling of unsaturated concrete. This is probably related to technical difficulties in experimental testing for this material. This paper is composed of two parts. In the first one, an original laboratory testing is developed. A prismatic bar is dried through its four lateral faces during one year. Then a cubic sample is cut from the central part of the prism and submitted to hydrostatic compression. The results obtained clearly show the induced mechanical anisotropy due to drying shrinkage. The second part is devoted to formulation of an elastoplastic model coupled with anisotropic damage. The proposed model is implemented into a FEM code by using fully coupled and implicit algorithm. Simulations of laboratory tests are provided to show that the proposed model is able to describe the main features related to coupled plastic damage behaviour of concrete, induced anisotropy, volumetric dilatancy, deterioration of elastic properties. One application example is finally presented.

2 EXPERIMENTAL RESULTS

In this section, a summary of experimental investigation is presented. The main objective of laboratory tests is to study anisotropic mechanical

behaviour induced by drying process. Therefore, each test is composed of two phases, drying phase and mechanical loading. A classic concrete with a Water by Cement ratio equal to $W/C = 0.6$ has been used. Prismatic specimens of dimensions $40 \times 40 \times 160 \text{ mm}^3$ were prepared and preserved in water during 28 days. Then, they were preserved in a hygrometry of 60% and under constant temperature. Drying of concrete occurs by the 4 lateral faces of prismatic bar (Figure 1). Measuring of specimen total weight loss and drying shrinkage, which is calculated from deformations of the extreme faces of prism, was carried out regularly during time. After one year of drying in these conditions, a cube of 40 mm was catted from the previous prism, in such a way that the cube has 4 faces (on the lateral faces of the prism) having undergone to drying process and two other faces (cross sections of the prism), obtained by sawing, being perpendicular to the privileged directions of desiccation (Figure 1 and 2).

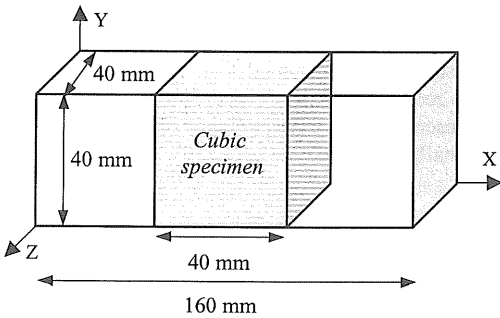


Figure 1: Cubic specimen cut from $40 \times 40 \times 160 \text{ mm}^3$ bar

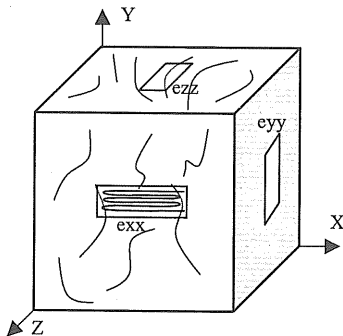


Figure 2: Illustration of microcracks on cubic sample and placement of strain gauges on each face

Three drying tests have been performed in same conditions to insure reliability of results. From each dried bar, a cubic sample is cut, which is submitted to hydrostatic compression test. Every face of this cube is instrumented by a strain gauge. Strains in

three orthogonal orientations are then measured to put in evidence the induced anisotropic mechanical responses after drying shrinkage of concrete. These hydrostatic compression tests were performed until 60 MPa. In Figure 3, typical strain curves versus hydrostatic stress are shown.

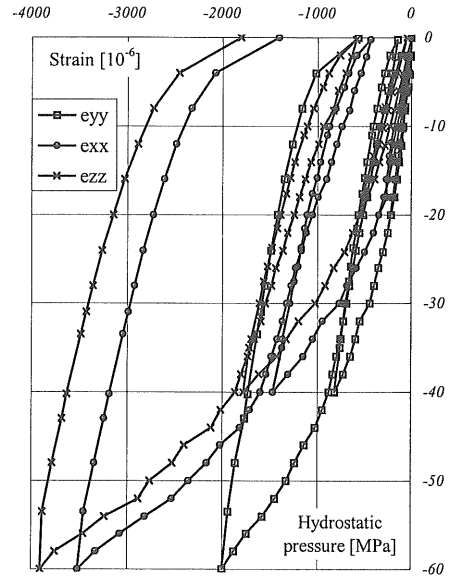


Figure 3: Typical strain curves versus hydrostatic stress in three orthogonal orientations (see Figure 2) (each strain is the average value of two parallel gauges in opposite faces)

First, we can see that three strains are non linear versus applied hydrostatic. Such non linear responses may be due to progressive closure of microcracks induced during drying phase at low value of stress, and due to plastic behavior of concrete under high level of stress. Further and in a more important manner, the strains obtained on the faces subjected to the drying condition (plans respectively normal to Y and Z axes) are much more important (nearly 1.5 to 2 times) than those obtained on the virgin faces of cube (plans normal to X axis). This difference clearly shows that oriented microcracks are induced during drying shrinkage, and they are mainly organized according to plans tangents to the main direction of the hydrous gradient.

3 CONSTITUTIVE MODELLING

This section is devoted to the formulation of the constitutive model for concrete in partially saturated condition. The model is formulated in the framework of thermodynamics of open systems. The porous medium is assumed to be saturated by a liquid

phase (noted by index w) and a gas mixture phase (noted by index g). The gas mixture is composed of dry air and water vapour. The state variables to be used are the strain tensor of skeleton frame ε_{ij} , the volumetric change of water content ($\phi_w - \phi_{w0}$) and gas content ($\phi_g - \phi_{g0}$), the damage variable D , the internal state variables for plastic hardening χ_k and the temperature T . In this work, the induced anisotropic material damage is described by a second rank tensor. When unilateral effect due to crack closure is neglected, the use of such a tensor is reasonable to represent orientation and density of microcracks. The damage tensor can be expressed with its three eigenvalues and eigenvectors by using spectral decomposition:

$$D = \sum_{k=1}^3 D_k V^k \otimes V^k \quad (1)$$

Further, the following partition rules are assumed :

$$\varepsilon_{ij} = \varepsilon_{ij}^e + \varepsilon_{ij}^p, \quad \phi_w - \phi_{w0} = \phi_w^e + \phi_w^p,$$

$$\phi_g - \phi_{g0} = \phi_g^e + \phi_g^p \quad (2)$$

The application of the thermodynamics laws leads to the following fundamental inequality (Coussy 1995) :

$$\sigma_{ij} d\varepsilon_{ij} + p_g d\phi_g + p_w d\phi_w - S_s dT - d\Psi_s \geq 0 \quad (3)$$

where S_s and Ψ_s are respectively the entropy and free energy of skeleton material per unit initial volume of bulk material. The standard differentiation of the free energy function in (3) yields in the following state equations:

$$\sigma_{ij} = \frac{\partial \Psi_s}{\partial \varepsilon_{ij}^e}, \quad p_g = \frac{\partial \Psi_s}{\partial \phi_g^e}, \quad p_w = \frac{\partial \Psi_s}{\partial \phi_w^e},$$

$$S_s = - \frac{\partial \Psi_s}{\partial T} \quad (4)$$

The intrinsic dissipations due to plastic flow and damage evolution have to satisfy the fundamental inequality as follows:

$$\sigma_{ij} d\varepsilon_{ij}^p + p_g d\phi_g^p + p_w d\phi_w^p - \frac{\partial \Psi_s}{\partial \chi_k} d\chi_k - \frac{\partial \Psi_s}{\partial D_{ij}} dD_{ij} \geq 0 \quad (5)$$

The present study will be limited to isothermal conditions. The general constitutive equation for coupled elastic-plastic damage behaviour of partially

saturated material can be expressed in the following general form :

$$d\sigma_{ij} = C_{ijkl}^{bT}(D) d\varepsilon_{kl}^e - b(S_w dp_w + (1 - S_w) dp_g) \delta_{ij} \quad (6)$$

where $C^{bT}(D)$ is the tangent elastic stiffness tensor of damaged material, the parameter b denotes the Biot's coefficient of porous medium and S_w the water saturation degree (Coussy 1995, Coussy et al. 1998). The micromechanical interpretation of the effective stress concept involved in this equation has been discussed by Chateau & Dormieux (1998) by using homogenisation approach. The complementary laws for plastic deformation and damage evolution have to be defined. The particular form of such functions should be identified from relevant experimental data. This is discussed in the next sections.

3.1 Characterisation of plastic deformation

In the case of partially saturated materials, experimental results have shown that plastic deformation can develop due to the variation of suction under constant stresses (Alonso et al. 1987, Alonso et al. 1990). Therefore, two distinct plastic mechanisms are usually identified, namely stress controlled and suction controlled plastic deformations. Furthermore, the stress controlled plastic deformation is generally influenced by water saturation degree. In this study, we are interested in modelling of partially saturated hard rocks and concrete. Damage by microcracks is known as a principal deformation and failure mechanism in this kind of materials. Therefore, we propose to use an elastic-plastic damage model. However, in order to make the formulation of model as simple as possible, classic functions are used for characterisation of plastic deformation.

The yield function for stress controlled plastic deformation is based on the Drucker-Prager criterion :

$$f_\sigma = q g(\theta) + \alpha_p (p'^p - C_s^p) = 0 \quad (7)$$

$$q = \sqrt{2J_2}, \quad \theta = \frac{1}{3} \text{Arc sin} \left[\frac{3\sqrt{3}}{2} \frac{J_3}{\sqrt{J_2^3}} \right],$$

$$J_2 = \frac{1}{2} S_{ij} S_{ij}, \quad J_3 = \det \mathbf{S}, \quad S_{ij} = \sigma_{ij} - \frac{\sigma_{kk}}{3} \delta_{ij} \quad (8)$$

where q is the deviatoric stress and θ the Lode's angle. The function $g(\theta)$ defines the dependency of yield condition on the third stress invariant. Its particular form can be identified from experimental

yield stresses on the deviatoric plane. Various forms are available in literature, for instance (Pietruszczak et al. 1988). However, for the reason of simplicity, we have taken in this work $g(\theta) = 1$.

The effect of capillary forces (moisture content) on stress controlled plastic mechanism is taken into account by definition of a generalised effective mean stress in plastic field, based on the Bishop concept in elastic field. It is expressed as follows:

$$p^{ip} = \frac{\sigma_{kk}}{3} + \beta [S_w p_w + (1 - S_w) p_g] = \frac{\sigma_{kk}}{3} + \beta [p_g - S_w p_c] \quad (9)$$

$p_c = p_g - p_w$

The material parameter β defines the contribution of capillary pressure p_c to the effective mean stress involved in the plastic yield criterion. The parameter C_s^p appears as material cohesion in saturated conditions when $S_w = 1$ (or $p_c = 0$).

In coupled plastic damage modelling, induced damage is considered as responsible to material softening of material. The plastic strain hardening of material is then described by the increasing function α_p , which is chosen as a function of the total equivalent plastic strain $\bar{\varepsilon}_p$. Based on experimental data, the following particular form is used:

$$\alpha_p = \alpha_r^p - (\alpha_r^p - \alpha_0^p) e^{-b \bar{\varepsilon}_p} \quad (10)$$

$$\bar{\varepsilon}_p = \int (d\varepsilon_{ij}^p d\varepsilon_{ij}^p)^{1/2}$$

The parameters α_0^p and α_r^p are respectively the initial and ultimate value of the hardening function and b controls the kinetics of plastic hardening.

Most experimental results obtained from cohesive frictional geomaterials (rocks and concrete) suggest that a non-associated plastic flow rule is generally needed. The following simple potential is used in this work:

$$g_\sigma = q g(\theta) + \beta_p p'^p \quad (11)$$

The constant parameter β_p controls plastic volumetric dilatancy of material.

The suction controlled plastic deformation is assumed to be a spherical tensor. It is used to describe plastic compaction and swelling of material due to suction change under constant stresses. Further, an associated flow rule is usually adopted. Based on the

previous works, for instance (Alonso et al. 1990), the following functions are retained :

$$f_s = p_c - s^p (\varepsilon_v^p) = 0 \quad , \quad g_s \equiv f_s \quad (12)$$

The corresponding plastic hardening is a function of the total plastic volumetric strain ε_v^p :

$$s^p = s_0^p e^{c\varepsilon_v^p} \quad (13)$$

The parameter s_0^p defines the initial yield threshold and c controls plastic hardening rate for suction controlled plastic flow. Figure 1 shows a schematic view of the yield surfaces in the (p, q, p_c) space.

The total plastic strain increment $d\varepsilon_{ij}^p$ is then calculated from the contributions of two mechanisms :

$$d\varepsilon_{ij}^p = d\varepsilon_{ij}^{p\sigma} + \frac{1}{3} d\varepsilon_v^{ps} \delta_{ij} = \Delta\lambda_\sigma \frac{\partial g_\sigma}{\partial \sigma_{ij}} - \Delta\lambda_s \frac{1}{3} \frac{\partial f_s}{\partial p_c} \delta_{ij} \quad (14)$$

Two plastic multipliers $\Delta\lambda_\sigma$ and $\Delta\lambda_s$ are obtained through plastic consistency conditions.

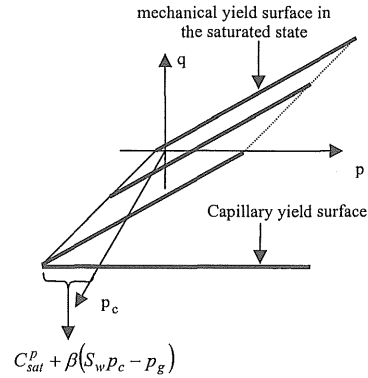


Figure 1 : A schematic view of stress and suction controlled yield surfaces in (p, q, p_c) space.

3.2 Characterisation of induced damage

Induced anisotropic damage is characterized by a second rank tensor. The effective elastic properties of damaged material is derived from the elastic free energy function. By assuming small density and no interaction of microcracks, the expression of free energy function may be obtained from micromechanics analysis of cracked solids (Pensee & Kondo 2001). When only open microcrack is considered, the elastic free energy can be approximated by:

$$\begin{aligned}
W^e(\varepsilon^e, D) &= \frac{\lambda_0}{2} (tr \varepsilon^e)^2 + \mu_0 tr(\varepsilon^e : \varepsilon^e) \\
&+ a_1 tr \varepsilon^e tr(\varepsilon^e : D) + a_2 tr(\varepsilon^e : \varepsilon^e : D) \\
&+ a_3 tr D (tr \varepsilon^e)^2
\end{aligned} \quad (15)$$

where λ_0 and μ_0 are the elastic constants of undamaged state. Three parameters a_1 , a_2 and a_3 determine deterioration of elastic properties due to damage. By standard differentiation, the elastic stiffness tensor of damaged dry material, $C^b(D)$, is obtained:

$$\begin{aligned}
C_{ijkl}^b(D) &= \lambda_0 \delta_{ij} \delta_{kl} + \mu_0 (\delta_{ik} \delta_{jl} + \delta_{il} \delta_{jk}) \\
&+ a_1 (\delta_{ij} D_{kl} + D_{ij} \delta_{kl}) \\
&+ \frac{a_2}{2} [\delta_{ik} D_{jl} + \delta_{il} D_{jk} + D_{ik} \delta_{jl} + D_{il} \delta_{jk}] \\
&+ 2a_3 tr D \delta_{ij} \delta_{kl}
\end{aligned} \quad (16)$$

In the framework of thermodynamics, the damage evolution law should be determined by formulation of pseudo dissipation potential as a function of conjugated forces associated to damage variable. Such a potential is usually complex to formulate and its experimental validation is not easy. In this work, a pragmatic approach is preferred, based on experimental observations. In brittle materials, it is observed that induced damage is inherently related to tensile strains. Further, coupled plastic damage behaviour, damage is emphasised by plastic strain. Therefore, the following simple damage criterion is proposed for concrete:

$$\begin{aligned}
f_d(\varepsilon, D) &= \sqrt{\varepsilon^{e+} : \varepsilon^{e+}} + \sqrt{\varepsilon^{p+} : \varepsilon^{p+}} \\
-(r_0 + r_1 tr D) &\leq 0
\end{aligned} \quad (17)$$

where r_0 and r_1 are two parameters controlling respectively initial damage threshold and damage evolution rate. Two tensors, ε^{e+} and ε^{p+} , are respectively positive (tensile) cones of elastic and plastic strain tensor. They are determined from the following spectral decomposition by Ortiz (1985) and Ju (1989):

$$\varepsilon^{e+} = \sum_{k=1}^3 \varepsilon_k^e H(\varepsilon_k^e) \mathbf{V}^{ek} \otimes \mathbf{V}^{ek} \quad (18a)$$

$$\varepsilon^{p+} = \sum_{k=1}^3 \varepsilon_k^p H(\varepsilon_k^p) \mathbf{V}^{pk} \otimes \mathbf{V}^{pk} \quad (18b)$$

where $H(\varepsilon_k)$ is the Heaviside step function of the k^{th} principal elastic or plastic strain ε_k and \mathbf{V}^k the

corresponding principal vector. Further, it is assumed that increment of damage tensor is co-axial with the superposition of positive cones of elastic and plastic strain:

$$dD = \lambda_d \frac{\varepsilon^{e+} + \varepsilon^{p+}}{\sqrt{\varepsilon^{e+} : \varepsilon^{e+}} + \sqrt{\varepsilon^{p+} : \varepsilon^{p+}}}$$

if $f_d = 0$ and $\dot{f}_d = 0$ (19)

The damage multiplier λ_d should be determined by the consistence condition of damage criterion.

3.3 Parameter identification and test simulation

The parameters involved in the constitutive model can be determined from experimental data obtained in uniaxial and triaxial compression tests. The table 1 gives the representative set of parameters for a concrete. The proposed model is implemented in the finite element code MPPSAT, which is able to solve coupled hydro-mechanical problems in partially saturated porous media. In Figure 4a, numerical simulation of an uniaxial compression test is compared with experimental data. There is a good agreement. In Figure 4b, deterioration of elastic stiffness in axial and lateral directions is presented as a function of lateral strain. The difference between two orientations shows that the model is able to describe induced anisotropic damage observed in experimental data.

Table 2 : Representative values of parameters used in simulations

Plastic parameters	Damage parameters	Physical parameters
$\beta = 0.4$	$r_0 = 0.0$	$\phi_0 = 0.35$
$\alpha_0^p = 0.1$	$r_1 = 8.76^{-4}$	$k = 1.10^{-18} m^2$
$\alpha_1^p = 1.65$	$a_1 = 9244 MPa$	$\rho_s = 2500 kg/m^3$
$b = 1000$	$a_2 = -14090 MPa$	$fvck = 1.10^{-7} m^2/s$
$C_s^p = 20 MPa$	$\alpha_3 = 0$	$T = 294 K$
$\beta^p = 0.6$	Elastic parameters	
$s_0^p = 9.5 MPa$	$E = 37100 MPa$	
$c = -1000$	$\nu = 0.31$	

By using these parameters, drying process and hydrostatic compression test of cubic sample are simulated. The objective is to show anisotropic mechanical behavior induced by drying shrinkage. The actual problem is then simplified and studied in

plane strain conditions. The geometry and boundary conditions are shown on Figure 5 and 6, respectively for drying and compression phases.

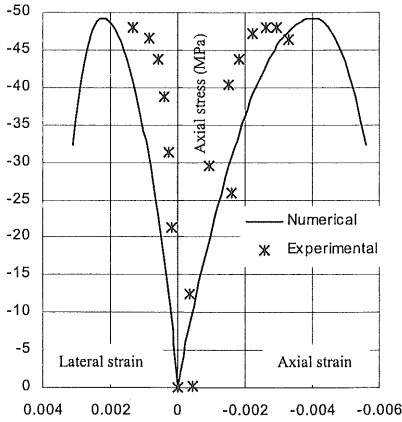


Figure 4a: Simulation of an uniaxial tension test

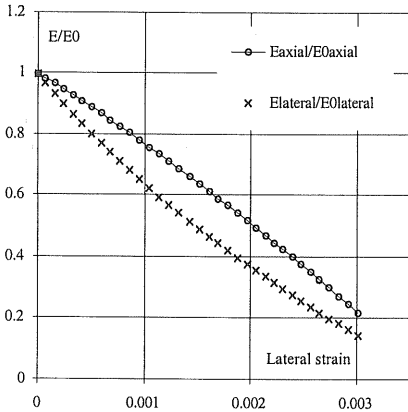


Figure 4b : Deterioration of elastic stiffness in axial and lateral directions as function of lateral strain

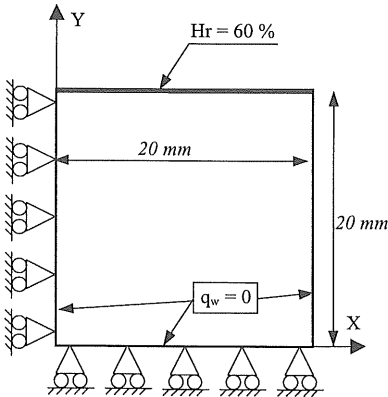


Figure 5: 1/4 of Cubic specimen simulation in 2D case (Step 1 : drying)

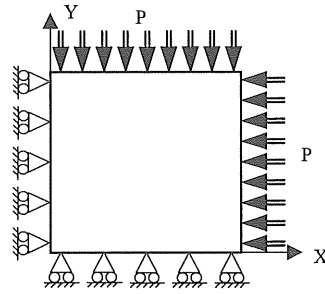


Figure 6: 1/4 of Cubic specimen simulation in 2D case (Step 2 : hydrostatique compression)

In figure 7, water saturation degree along the height of cube (direction of drying process) at 70 days is shown. We have still a non uniform desaturation in the cube. Two normal strains due to hydrostatic compression are presented on Figures 8 for two points on the faces of cube. Notice that material responses during hydrostatic compression should be elastic, because unilateral effect and plastic behavior due to hydrostatic loading are not taken into account in the current version of the model. The difference between the two normal strains indicates an induced anisotropic elastic behavior of the material. In this work, we don't attempt to make quantitative comparison with experimental data. This will be done by making 3D modeling.

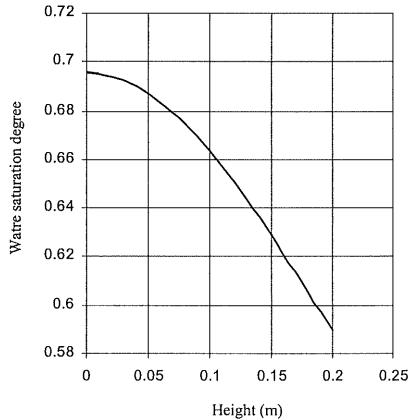


Figure 7: Water saturation degree along height (direction of drying)

4 APPLICATION EXAMPLE

In this section, a typical example concerning drying shrinkage of concrete structure is studied by using the proposed model. All calculations are made by using the finite element code MPPSAT. A fully coupled algorithm and an implicit time increment scheme are used in this code. The numerical simula-

tion have been performed with the following water retention curve (Lassabatère 1994) :

$$S_{wv} = [1 + (a p_c)^b]^c, \quad a = 2.346 \times 10^{-8}, \quad b = 0.827, \quad c = -0.5767 \quad (20)$$

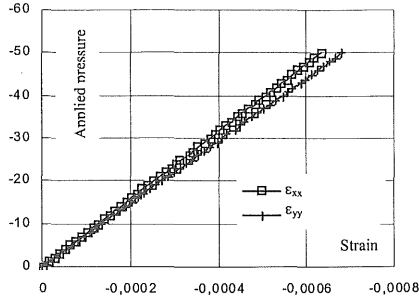


Figure 8a: Normal strains due to hydrostatic compression on the point A

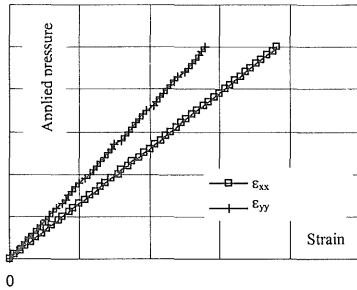


Figure 8b: Normal strains due to hydrostatic compression on the point B

We consider a cylinder column submitted to drying through its lateral face. The geometry and loading conditions are given on Figure 9. According to symmetry of the problem, only quarter of the column is considered. Figure 10 shows profiles of water

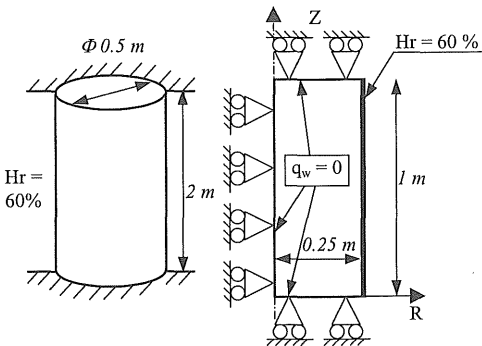


Figure 9 : Geometry and boundary conditions of cylinder column

saturation degree along the radius of cylinder for different times. We notice that a nearly uniform drying state is obtained after 120 days. On figure 11, we present distributions of two damage components (radial and axial) along the radius at the middle height at 120 days. The axial damage is much higher than the radial one. Therefore, the induced damage is clearly anisotropic and microcracks are essentially oriented in radial direction.

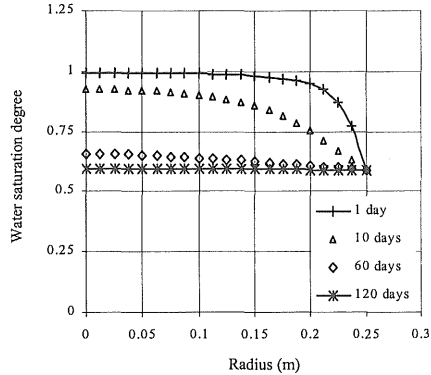


Figure 10: Water saturation degree along the radius of cylinder as functions of time

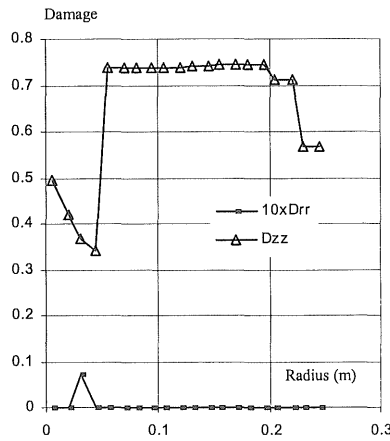


Figure 11: Distribution of damage components at the middle height of cylinder at 120 days

4. CONCLUSIONS

An original experimental testing is proposed and the results obtained have clearly shown induced anisotropic mechanical behaviour by drying shrinkage. An coupled elastoplastic damage model is proposed for modelling of hydro-mechanical behaviour of partially saturated concrete. Anisotropic damage is

described by a second rank tensor. The proposed model is quite simple and easy to be identified. Numerical simulations of laboratory tests have shown that the model is able to describe basic characteristics related to induced anisotropic damage in concrete, due to either mechanical loading and drying shrinkage. One application example has been studied by using the proposed model implemented in a FEM code. Anisotropic damage due to drying shrinkage is put in evidence.

REFERENCES

- Alonso E.E., Gens A. & Hight D.W., 1987, Special problem soils. General report. Proc. 9th European Conf. Soil Mech. And Foundation Engng. Dublin, Vol.3, Balkema, 1087-1146.
- Alonso, E. E., Gens, A. & Josa, A., 1990, 'A constitutive model for partially saturated soils.' *Géotechnique* 40 (3), 405-430.
- Bazant, Z.P. & Wittmann, F.H. 1982, *Creep and Shrinkage in Concrete Structures*, J. Wiley and Sons.
- Chateau X. & Dormieux L., 1998, 'A micromechanical approach to the behavior of a non-saturated porous medium', *C.R. Acad. Sci. Paris*, t326, Série II b, 533-538
- Colina, H. & Acker, P. 2000. Drying cracks and scale laws, *Materials and structures*, 33, 101-107
- Coussy, O., 1995, 'Mechanics of porous continua.', J. Wiley&Sons.
- Coussy O., Eymard R. & Lassabatère T., 1998, 'Constitutive modelling of unsaturated drying deformable materials', *J. of Engineering mechanics* 124 (6), 658-667.
- Lassabatère T., 1994, 'Couplages hydromécaniques en milieu poreux non saturé avec changement de phase : Application au retrait de dessiccation', Thèse de doctorat de l'Ecole Nationale des Ponts et Chaussées, Paris.
- Mazars J., 1984, 'Application de la mécanique de l'endommagement au comportement non linéaire et à la rupture du béton de structure.', Thèse de Doctorat d'Etat de l'Université Paris 6.
- Pietruszczak S., Jiang J. & Mirza F.A., 1998, 'an elastoplastic constitutive model for concrete.', *Int J. Solids & Structures* 24 (7), 705-722.
- Wittmann F.H., 'Le séchage et le retrait de dessiccation du béton', Proc. of Expérimentation et Calcul en Génie Civil, EC97, Strasbourg, France, (1997) 15-26